CHEMISTRY
A European Journal

A Journal of
ChemPubSoc Europe

Accepted Article

Title: Fullerene-Based Materials as Hole-Transporting/Electron Blocking Layers. Applications in Perovskite Solar Cells

Authors: Juan L. Delgado, Luis E. Hueso, Elisabetta Zuccatti, Silvia Collavini, Sebastian F. Völker, Jorge Pascual, Ramón Tena-Zaera, Marta Vallés-Pelarda, Iván Mora-Seró, and Fernando Ruiperez

To be cited as: *Chem. Eur. J.* 10.1002/chem.201801069

Link to VoR: http://dx.doi.org/10.1002/chem.201801069

Supported by
ACES

WILEY-VCH

10.1002/chem.201801069

COMMUNICATION

WILEY-VCH

Fullerene-Based Materials as Hole-Transporting/Electron Blocking Layers. Applications in Perovskite Solar Cells

Sebastian F. Völker,[a]+ Marta Vallés-Pelarda,[b]+ Jorge Pascual,[c,a] Silvia Collavini,[a] Fernando Ruiperez,[a] Elisabetta Zuccatti,[d] Luis E. Hueso,[d,e] Ramón Tena-Zaera,*[c] Iván Mora-Seró,*[b] and Juan Luis Delgado*[a,e]

Dedicated to Prof. Dr. Christoph Lambert on the occasion of his 50th birthday

Abstract: *Here we report for the first time an efficient fullerene-based compound, **FU7**, able to act as Hole-Transporting Material (HTM) and electron blocking contact. It has been applied on perovskite solar cells (PSCs), obtaining 0.81 times the efficiency of PSCs with the standard HTM, spiro-OMeTAD, with the additional advantage that this performance is reached without any additive introduced in the HTM layer. Moreover, as a proof of concept, we have described for the first time efficient PSCs where both selective contacts are fullerene derivatives, to obtain unprecedented "fullerene sandwich" PSCs.*

Since the discovery of fullerene, this molecule and the myriad of its synthesized derivatives have played a key role in the development of organic electronics.[1] Fullerenes or fullerene monoadducts, such as the well-known [6,6]-phenyl C_{61} butyric acid methyl ester (PCBM), display a suitable LUMO level (–4.03 eV)[2a] to act as good electron-transporting material (ETM), for example in the ideal working principle scheme of organic or perovskite solar cells.[3] Moreover, their soft processing conditions (low temperature, solution-processed), thermal stability and ability to transport charge allow their integration in low cost optoelectronic devices. For all these reasons it is generally established that fullerenes are outstanding electron transporters and excellent hole blockers. However, the use of a suitable chemical design combined with the intrinsic chemical versatility of fullerenes can prove that this general assumption could be revisited as we show in this work. [60]fullerene hexakis adducts have been employed recently as scaffolds to prepare liquid crystalline materials, non-viral gene delivery systems and bioactive glycoclusters.[4] However, to the best of our knowledge, [60]fullerene hexakis adducts remain unexplored in the field of solar cells, being the present study the first successful incorporation of these materials on efficient PSCs.

The addition of six organic addends to the fullerene cage to afford [60]fullerene hexakis adducts induces dramatic changes in their LUMO energy level.[5] Indeed, [60]fullerene hexakis adducts present a very different LUMO energy value (up to one volt) compared with fullerene monoadducts. Considering all these points, in the present paper we have prepared a novel [60]fullerene hexakis adduct **FU7**, suitably functionalized with twelve "*super-triarylamine*" fragments, in order to warrant the hole-transporting ability of this new material (Figure 1). **FU7** was obtained by 12-fold Cu-catalyzed alkine-azide "click" reaction between the pre-constructed C_{60} building block[4e] bearing 12 azide groups and "*super-triarylamine*" **TAA14** (Scheme S3). The chemical identity of **FU7** was unambiguously confirmed by several spectroscopic techniques (Methods section and Figures S1-S21).

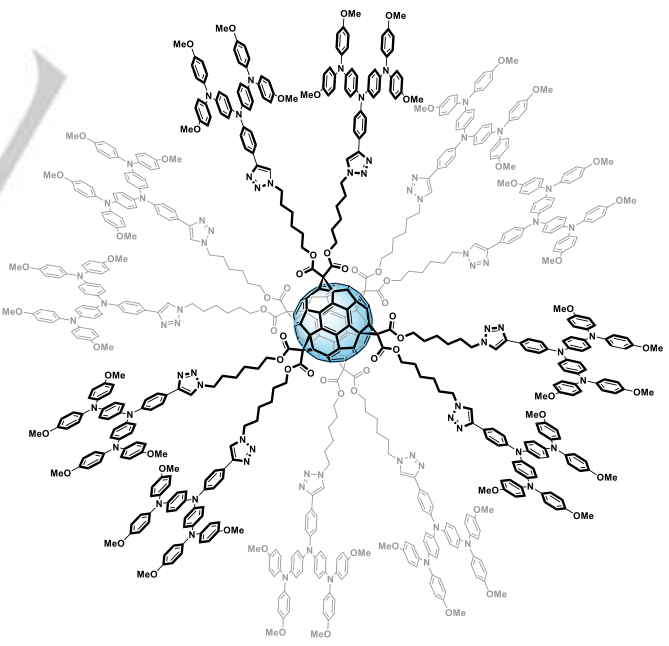

Figure 1. Chemical structure of novel [60]fullerene hexakis adduct **FU7**.

The electronic properties of **FU7** were investigated by means of cyclic voltammetry (Figure S22) and differential pulse voltammetry in methylene chloride (Figure S23), allowing to estimate a HOMO value of –5.04 eV and a LUMO value of –3.50 eV. This fact represents a significant reduction of electron affinity

[a] Dr. S. F. Völker, J. Pascual, S. Collavini, Dr. F. Ruiperez, Prof. J. L. Delgado
POLYMAT, University of the Basque Country UPV/EHU.
Avenida de Tolosa 72, 20018 Donostia-San Sebastián, Spain.
E-mail: juanluis.delgado@polymat.eu
[b] M. Vallés-Pelarda, Dr. I. Mora-Seró
Institute of Advanced Materials (INAM), University of Jaume I.
Av. de Vicent Sos Baynat, s/n 12006, Castelló de la Plana, Spain.
E-mail: sero@fca.uji.es
[c] J. Pascual, Dr. R. Tena-Zaera
Materials Division, IK4-CIDETEC
Parque Tecnológico de San Sebastián, Paseo Miramón, 196,
Donostia – San Sebastián 20009, Spain.
E-mail: rtena@cidetec.es
[d] E. Zuccatti, Prof. L. E. Hueso
CIC nanoGUNE Consolider, 20018 Donostia – San Sebastián, Spain
[e] Prof. L. E. Hueso, Prof. J. L. Delgado
Ikerbasque, Basque Foundation for Science, 48011 Bilbao, Spain.
+ Both authors have contributed equally to this work.

Supporting information for this article is given via a link at the end of the document.

in respect to the well-established fullerene-based ETM LUMO level (e.g., –4.03 for PCBM, Figure S22). [2a] Density functional theory (DFT) calculations carried out with Gaussian 096[6] indicated that the HOMO is located on the super-triarylamine hole-transporting fragments and the LUMO is located on the fullerene cage (Figure S31). Furthermore, the study of non-optimized OFET devices constituted of Si/SiO_2(150nm)/HMDS/Ti(5nm)/Au(35nm)/**FU7** allowed to confirm that **FU7** is a p-type semiconductor, which displays lower hole mobility than reference spiro-OMeTAD (Figure S32-S33). The LUMO level of **FU 7** (-3,5 eV), is comparable to other HTMs which have been described as efficient electron blocking materials. [2b-d]

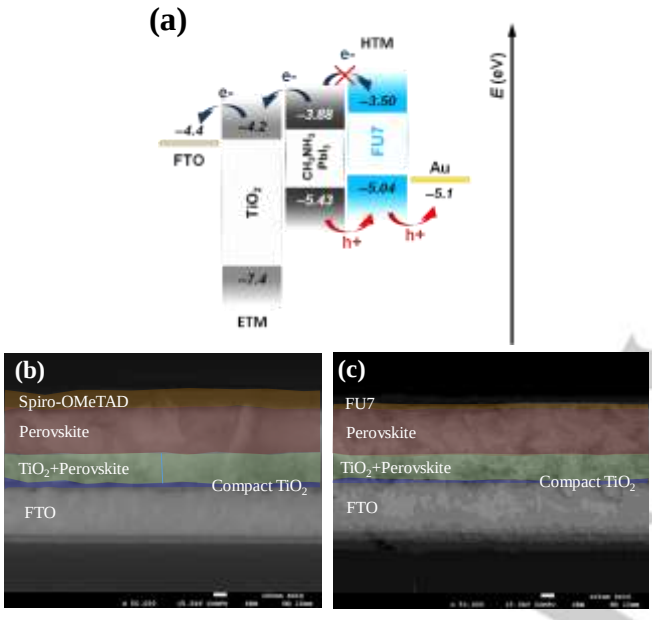

Figure 2. (a) Ideal working principle scheme of PSCs. (b) and (c) respectively cross section of PSC using spiro-OMeTAD and **FU7** as HTM, with compact TiO_2 as electron selective contact and mesoporous TiO_2 scaffold. Scale bar indicates 100 nm.

Thus, considering the ideal working principle scheme of PSCs (Figure 2a), the energy levels estimated by electrochemistry and DFT (Figures S22, S23 and S31), as well as p-type character of **FU7** confirmed by OFET measurements, this novel fullerene-based material is an ideal candidate to behave as an electron-blocking/hole-transporting material in PSCs.[7] It is important to remark that, with the addition of six organic "supertriarylamine" fragments, we are able to modulate the HOMO and LUMO of **FU7** in a single step. Thus, the LUMO of **FU7** (–3.50 eV) is almost 0,40 eV more positive than the LUMO of perovskite (Figure 2a), therefore this fullerene material is able to efficiently block electrons and suitable to behave as efficient hole-selective layer. Taking into account the ideal working principle of perovskite solar cells, illustrated on Figure 2a, the LUMO value of PCBM (-4,02 eV) would not be suitable to block electrons, being this layer not selective to the transport of holes.

Fullerenes have been extensively proposed in the field of organic solar cells (OSCs),[8] and more recently in PSCs, showing excellent photovoltaic behavior and improving PSCs stability.[9] In particular, they have been mainly used as ETMs,[3a] but also as additives in the perovskite layer.[10,11] The use of fullerene and fullerene-based molecules in PSCs have helped reducing hysteresis,[12,13] contributed to efficiency enhancement[11] and increased long-term stability.[10,14] These benign effects have been reached by passivating the interfaces of PSCs and grain boundaries of perovskite and by acting as excellent hole-blocking ETL. In the case of **FU7**, due to the above-mentioned properties, a new role can be envisaged for the first time by a fullerene-based derivative.

To corroborate this hypothesis, PSCs were prepared using **FU7** as HTM and compared to standard reference (Ref) cells using spiro-OMeTAD (Figure 3a), which has been the first HTM employed in all-solid PSCs[15,16] and the current most extensively used HTM. PSCs have been prepared using glass, coated with fluorine-doped SnO_2 (FTO) as transparent conductive contact. A compact layer of TiO_2 deposited by spray pyrolysis, with ~50 nm thickness, has been used as electron selective contact, with a mesoporous layer, ~200 nm, deposited on top. After the $CH_3NH_3PbI_3$ perovskite deposition in air conditions[17] a capping layer of perovskites of ~300 nm was formed on top of mesoporous layer (Figures 2b and 2c). As HTM, both spiro-OMeTAD and **FU7** have been used. Ref cells present efficiencies in the average of the reported ones in the literature considering that $CH_3NH_3PbI_3$ is used as active layer (Table S2). The optimum conditions of concentration for the deposition of **FU7** dissolved in chlorobenzene have been evaluated (Table S1 and Figure S24), observing that the highest efficiencies were obtained with concentrations of 8-9 mg ml^{-1}. Such concentrations produce a layer of **FU7** with ~40 nm thickness (Figure 2c), sensibly smaller than the standard ~200 nm spiro-OMeTAD layer (Figure 2b). Higher concentrations produced thicker films, increasing the hole transport resistance at the HTM as it has been analyzed by Impedance Spectroscopy (IS) (Figure S25).[18] A reduction of concentration produced too thin layers with pinholes.

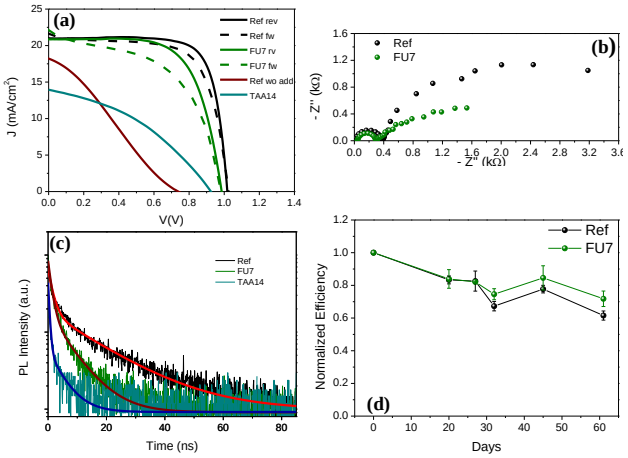

Figure 3. (a) Current-potential (*J-V*) curves without any preconditioning of champion reference (Ref) cell (using spiro-OMeTAD with additives as HTM)

and a cell with **FU7** additive-free as HTM. Curves at forward (fw) and reverse (rv) scans are plotted. For comparison, fw scan of a solar cell prepared with spiro-OMeTAD but without any additive and a cell using the **TAA14** functional groups as HTM are included. (b) Nyquist plot of Ref and **FU7** cell under 1 sun illumination at 0.6 V DC forward applied bias. (c) The time-resolved photoluminescence (TRPL) response acquired using time-correlated single-photon counting (TCSPC) technique, 456 nm has been used as excitation wavelength and signal has been detected at 770 nm, maximum of the PL detected for the perovskite layer. The decays have been fitted with double exponential functions, which are plotted as solid lines. (d) Normalized efficiency obtained from the average of three cells at each condition (using spiro-OMeTAD and **FU7** as HTM), cells without any encapsulation were stored under dark in dry air atmosphere.

The maximum efficiency obtained for a PSC with the architecture plotted in Figure 1c has been 13.7% using a concentration of 9 mg ml^{-1} of **FU7** (Table S2). With this concentration, the perovskite layer is coated as a uniform and smooth layer with no pinholes covering the perovskite film (Figure S26). We have verified that the stabilized efficiencies are very close to the efficiencies obtained with the *J-V* curve from the reverse scan (Figure S27). Champion device prepared with spiro-OMeTAD at the same conditions reports a photoconversion efficiency of 16.9%. *J-V* curves for champion cells prepared with **FU7** and spiro-OMeTAD are depicted in Figure 3a. It is important to highlight, that spiro-OMeTAD needs additives to work properly as HTM, concretely 4-tert-butylpyridine (TBP) and lithium bis(trifluoromethane) sulfonimidate (LiTFSI) have been used as additives, for spiro-OMeTAD preparation. Without these additives, the performance of the devices prepared with spiro-OMeTAD as HTM decreases dramatically (Figure 3a, Table S2). However, no additive was employed for the preparation of solar cells employing **FU7** as HTM.[19] The use of additives to increase the conductivity of HTM has some important drawbacks, being the reduction of long-term stability the most important one.[20,21] In this sense, a great effort has been carried out to develop additive-free HTMs. Despite this effort, no additive-free system has surpassed the performance obtained with reference cells with doped spiro-OMeTAD. The highest efficiency reported for an additive-free HTM has been obtained with a molecularly engineered star-shaped D–π–A molecule incorporating a rigid quinolizino acridine.[20] To this extent, the efficiency obtained with **FU7** is especially significant, since this derivative is the first fullerene-based material able to act as hole selective layer, with an average efficiency of 0.77±0.05 times (0.81 times for champion cells) the efficiency of reference cells, comparing more than 70 cells of each kind.

In order to understand the different performance of **FU7** in comparison to reference cell, electrical (impedance spectroscopy (IS)) and optical (Time resolved photoluminescence (TRPL)) characterization have been carried out. A representative Nyquist plot for both HTM is depicted in Figure 3b. It can be clearly appreciated that the low frequency arc is bigger for the reference sample. This arc is associated with the recombination resistance,[18,22,23] being inversely proportional to the recombination rate. Consequently, IS points to a higher recombination reducing the photovoltage in the cell containing **FU7** instead of spiro-OMeTAD, in good agreement with the experimental data (Figure 3a). This point is confirmed by TRPL measurements (Figure 3c). The pattern obtained with TRPL has been fitted using a biexponential decay as it has been previously reported in the literature.[24-26] The value of the obtained characteristic times is depicted in Table S3. A faster decay of PL is observed when **FU7** is deposited on top of the perovskite layer. Two characteristic times τ_1 and τ_2 have been obtained from the fitting. The fastest one, τ_1, is associated with the charge carrier injection into HTM, whereas the slowest one, τ_2, is associated with recombination.[24-26] Deposition of **FU7** layer on top of perovskite reduces τ_1 significantly indicating an efficient hole transfer. However, recombination is also faster as it can be deduced by the decrease of τ_2. This analysis points to the direction that fullerene-based HTMs have to reduce interfacial recombination[27] in the future so as to improve the performance here reported.

Another important aspect that needs further analysis is the real work of fullerenes in the hole-transporting properties of **FU7**. From Figure S31 it can be clearly recognized that holes at HOMO are localized in the super-triarylamine (TAA) moieties covalently connected to the fullerene. The TAA fragment is by itself susceptible of being employed as HTM because it presents an efficient hole-scavenging effect as it has been characterized by the low τ_1 measured by TRPL (Figure 3c and Table S3). **TAA14** is the chemical precursor of **FU7** which does not contain fullerene on its chemical structure (Scheme S3) thus, devices with pinhole-free **TAA14** films (Figure S27) as HTM have been prepared. However, the performance obtained with **TAA14** is significantly lower than the observed with **FU7** as HTM (Table S2 and Figure 3a). Two different aspects could contribute to the higher performance of **FU7** in comparison with **TAA14**. On the one hand, a higher recombination for **TAA14** HTM, comparing τ_2 values in Table S3. On the other hand, the presence of fullerenes provides **FU7** with a perfect spherical shape (Figure 1), allowing a good connection of HOMO among molecules and a good separation of LUMO, centered on fullerene (Figure S31). In addition, spherical shape permits the deposition of more ordered layers. It has been observed that PCBM layers with higher structural order present a lower energy disorder and a higher Fermi level splitting, producing as a result devices with higher photovoltages.[9,28]This fact points out a key role developed by fullerene in fullerene-based HTMs producing charge separation, easy transport pathway and structural order.

Finally, the potential of additive-free fullerene-based HTM has been analyzed in order to enhance the PSC stability. The hydrophobic character of fullerenes has contributed to increase long-term stability of PSCs[10,14]. The average efficiency of samples without any encapsulation stored in dry air conditions and under dark is plotted in Figure 3d. Three cells of each type, with spiro-OMeTAD and **FU7** as HTMs, have been measured during two months and the results averaged in Figure 3d. During the first month the samples reduced in average their efficiency to 0.85 times the initial value for both reference and **FU7** samples. However, during the second month the efficiency of reference samples was reduced to 0.61 times the original value while the efficiency of **FU7** samples was reduced in a less significant amount to 0.72 times the initial value. This decrease in performance is due to a different evolution of the cell parameters photocurrent (J_{sc}), photovoltage (V_{oc}) and fill factor (*FF*) (Figure S29). V_{oc} was kept constant for reference cells during the two months of the experiment while for **FU7** samples photovoltage increased to 1.05 times the initial value and then kept constant (Figure S29a). The decrease in *FF* was higher for reference

samples than for **FU7** cells (Figure S29b). Additionally, J_{sc} of **FU7** samples is reduced to 0.81 times the original value after ten days but this value did not further decrease during the rest of the experiment. However, the decrease in photocurrent registered for reference cells is more progressive, but attains the same level that the one of **FU7** cells after two months. This analysis indicates that, as fullerene-based ETMs, fullerene-based HTMs have also the potential of increasing PSC stability, especially if the initial decrease on J_{sc} can be controlled.

Moreover, as a proof-of-concept we have developed for the first time a PSC where both selective contacts are fullerene-based systems and the active layer itself also contains fullerenes (Figure 4a and Method section for further details about preparation). In this fullerene sandwich-perovskite device C_{60} and **FU7** were used as ETM and HTM, respectively. In addition, C_{60} has been used as additive in the perovskite layer processing to avoid C_{60} film degradation during the solar cell fabrication.[29] This fullerene device, despite it needs further optimization, presents a significant efficiency close to 9%. The achieved value for J_{sc} (15.8 mA cm^{-2}) was comparable to the reference device with spiro-OMeTAD as HTM prepared in the same device series (Figure S30). However, *FF* (62.5%) and V_{oc} (0.92 V), although decent, were significantly lower than those from spiro-OMeTAD reference device. It is worth noting that no levelling-effect was detected for **FU7** film in FE-SEM micrographs of the device cross-section (Figure 4a). This finding differs from the efficient levelling-effect provided by spiro-OMeTAD layer.[29] As the glass/FTO/C_{60}/perovskite samples used in this study exhibited significant roughness, the HTL–levelling effect may be crucial for the solar cell performance anticipating wide room for improvement in the current non-intensively optimized **FU7** devices. However, the reached power conversion efficiency can be considered as a first proof of concept of "fullerene sandwich" perovskite solar cells. Most importantly, there is plenty of room for further optimization based on deposition processes more suitable for newly synthesized fullerene-based HTMs, with enhanced properties in respect to the novel **FU7**. In this regard, the rich chemical versatility of [60]fullerene hexakis adducts will allow the introduction of a great variety of hole transporting fragments, such as porphyrins, phthalocyanines or exTTF, which could improve and surpass the photovoltaic performance reported here for **FU7**.[30,31] In addition, a proper evaluation of oxidizing additives for **FU7** could help for the conductivity improvement with a positive effect in the performance.

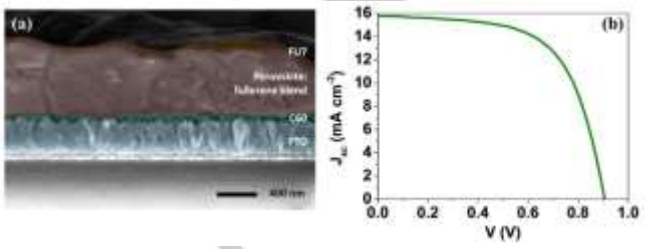

Figure 4. (a) Cross-section FE-SEM micrograph of a "fullerene sandwich" perovskite device with FTO/C_{60}/pvsk:C_{60}/**FU7**/Au architecture. Layers are colored for better discernment (FTO blue; C_{60} green; pvsk:C_{60} blend red; **FU7** brown). The local thickness of the fullerene layers depends on roughness of the layer on which they are deposited, being 10-40 nm for C_{60} and 10-50 nm for **FU7**. (b) *J-V* curve for champion solar device with "fullerene sandwich" architecture shown in (a), for comparison with reference cell see Figure S30**.**

In summary, we reported for the first time a HTM based on fullerenes. An appropriated chemical design has allowed tailoring the HOMO and LUMO levels of **FU7**, making it able to block electrons and act as hole selective contact. This molecule has been applied as HTM in PSCs without any additive. Significant efficiencies have been reported obtaining 0.77 in average (0.81 for champion devices) times the performance of the reference cell prepared with doped spiro-OMeTAD. In addition, cells prepared with **FU7** present higher stability than the reference cells. The presence of fullerenes play a structural key role in the HTM as it permits the formation of spherical molecules with charge separation, an easy transport pathway interconnection and an increase in the structural order of the film resulting on higher device performance. Finally, we have reported for the first time efficient "fullerene sandwich" PSCs where both selective contacts are fullerene-based systems and the active layer itself also contains fullerenes. Our results could have important implications in the development of a new branch in the family of fullerene derivatives, taking the advantage of the enormous knowledge already acquired in the synthesis of this kind of compounds but applying in a completely new field as HTL and electron blocking systems.

Acknowledgements

This work was partially supported by the MINECO of Spain (Grant Number CTQ2015-70921), Red Guipuzcoana de Ciencia, Tecnología e Innovación (MSFP) and European Research Council (ERC) via Consolidator Grant (724424 - No-LIMIT). J.P. and S.C. acknowledge the Basque Government for a PhD research grant. J.P. and J.L.D. acknowledge Iberdrola Foundation for financial support. We thank Carles Felip and Francisco Galindo from University Jaume I (UJI) for their help with TRPL measurements. We also thank Ivet Kosta (CIDETEC) for the FESEM characterization of the "fullerene sandwich" perovskite solar cells. We acknowledge SCIC from UJI for help with XRD and SEM characterization.

Keywords: Fullerenes • HTMs • PSCs • Fullerene-Sandwich PSCs

[1] a) C.-Z. Li, H.-L. Yip, A. K. Y. Jen, *J. Mater. Chem.* **2012**, *22*, 4161–4177; b) B. C. Thompson, J. M. J. Frechet, *Angew. Chem. Int. Ed*. **2008**, *47*, 58–77; c) J.-F. Nierengarten, *New J. Chem*. **2004**, *28*, 1177-1191; d) J.-F. Nierengarten, *Sol. Energy Mater. Sol. Cells* **2004**, *83*, 187–199.

[2] a) The LUMO levels of PCBM and **FU7** were estimated by CV or DPV under the same experimental conditions, using the following equation which is discussed on the SI (Experimental methods) *E* (HOMO/LUMO) = –5.16 eV – $E_{(oxidation/reduction)}$; b) M. Cheng, C. Chen, X. Yang, J. Huang, F. Zhang, B. Xu and L. Sun, *Chem. Mater*., **2015**, *27*, 1808–1814; c) S. Kazim, F. J. Ramos, P. Gao, M. K. Nazeeruddin, M. Grätzel and S. Ahmad, *Energy Environ. Sci*., **2015**, *8*, 1816–1823; d) C. H. Teh, R. Daik, Eng L. Lim, C. C. Yap, M. A. Ibrahim, N. A. Ludin, K. Sopiana, M. A. M. Teridi, | *J. Mater. Chem. A*, **2016**, *4*, 15788–15822.

[3] a) S. F. Völker, S. Collavini, J. L. Delgado, *ChemSusChem* **2015**, *8*, 3012-3028; b) S. Kazim, M. K. Nazeeruddin, M. Grätzel, S. Ahmad, *Angew. Chem. Int. Ed.* **2014**, *53*, 2812–2824; c) S. Collavini, S. F.

Völker, J. L. Delgado, *Angew. Chem. Int. Ed*. **2015**, *54*, 9757–9759; d) V. Dyakonov, J. L. Delgado, *Adv. Energy Mater*. **2017**, *7*, 1700252; S. Collavini, J. L. Delgado, *Adv. Energy Mater*. **2017**, *7*, 1601000.

[4] a) J.-F. Nierengarten, *Chem. Commun*. **2017**, *53*, 11855-11868; b) P. Fortgang, E. Maisonhaute, C. Amatore, B. Delavaux-Nicot, J. Iehl, J.-F. Nierengarten, *Angew. Chem. Int. Ed*. **2011**, *50*, 2364–2367; c) P. Compain, C. Decroocq, J. Iehl, M. Holler, D. Hazelard, T. Mena Barragán, C. Ortiz Mellet, J.-F. Nierengarten, *Angew. Chem. Int. Ed.* **2010**, 49, 5753–5756; d) A. Muñoz et al., *Nat. Chem.* **2016**, *8*, 50–57; e) J. Iehl, R. Pereira De Freitas, B. Delavaux-Nicot, J.-F. Nierengarten, *Chem. Commun*. **2008**, 2450–2452.

[5] a) C. Boudon, J.-P. Gisselbrecht, M. Gross, L. Isaacs, H. L. Anderson, R. Faust, F. Diederich, *Helv. Chim. Acta* **1995**, *78*, 1334–1344; b) L. Echegoyen, L. Echegoyen, *Acc. Chem. Res.* **1998**, *31*, 593–601.

[6] M. J. Frisch et al., *Gaussian 09, Revision A.1.*, Gaussian Inc., Wallingford CT, **2009**.

[7] W. S. Yang et al., *Science* **2017**, *356*, 1376-1379.

[8] J. L. Delgado, P.-A. Bouit, S. Filippone, M. A. Herranz, N. Martin, *Chem. Commun*. **2010**, *46*, 4853-4865.

[9] a) Y. Fang, C. Bi, D. Wang, J. Huang, *ACS Energy Lett.* **2017**, *2*, 782-794; b) C. Cui, Y. Li, Y. Li, *Adv. Energy Mater*. **2017**, *7*, 1601251; c) T. Gatti, E. Menna, M. Meneghetti, M. Maggini, A. Petrozza, F. Lamberti, *Nano Energy* **2017**, 41, 84–100.

[10] a) J. Pascual, I. Kosta, T. Tuyen Ngo, A. Chuvilin, G. Cabanero, H. J. Grande, E. M. Barea, I. Mora-Seró, J. L. Delgado, R. Tena-Zaera, *ChemSusChem* **2016**, *9*, 2679-2685; b) S. Collavini, M. Saliba, W.R. Tress, P. J. Holzhey, S. F. Völker, K. Domanski, S. H. Turren-Cruz, A. Ummadisingu, S. M. Zakeeruddin, A. Hagfeldt, M. Grätzel, J. L. Delgado, *ChemSusChem* **2018** doi:10.1002/cssc.201702265 ; c) R. Sandoval-Torrientes, J. Pascual, I. García-Benito, S. Collavini, I. Kosta, R. Tena-Zaera, N. Martín, J. L. Delgado, *ChemSusChem* **2017**, *10*, 2023.

[11] W. Wu, X. Yang, W. Chen, Y. Yue, M. Cai, F. Xie, E. Bi, A. Islam, L. Han, *Nat. Energy* **2016**, *1*, 16148.

[12] Y. Shao, Z. Xiao, C. Bi, Y. Yuan, J. Huang, *Nat. Commun.* **2014**, *5*, 5784.

[13] M. Valles-Pelarda, B. C. Hames, I. García-Benito, O. Almora, A. Molina-Ontoria, R. S. Sánchez, G. Garcia-Belmonte, N. Martín, I. Mora-Seró, *J. Chem. Phys. Lett.* **2016**, *7*, 4622-4628.

[14] Y. Bai, Q. Dong, Y. Shao, Y. Deng, Q. Wang, L. Shen, D. Wang, W. Wei, J. Huang, *Nat. Commun.* **2016**, *7*, 12806.

[15] H.-S. Kim et al., *Sci. Rep.* **2012**, *2*, 591.

[16] M. M. Lee, J. Teuscher, T. Miyasaka, T. N. Murakami, H. J. Snaith, *Science* **2012**, *338*, 643-647.

[17] C. Aranda, C. Cristobal, L. Shooshtari, C. Li, S. Huettner, A. Guerrero, *Sustainable Energy Fuels* **2017**, *1*, 540-547.

[18] E. J. Juarez-Perez, M. Wußler, F. Fabregat-Santiago, K. Lakus-Wollny, E. Mankel, T. Mayer, W. Jaegermann, I. Mora-Seró, *J. Chem. Phys. Lett.* **2014**, *5*, 680-685.

[19] The addition to **FU7** films of the same additives employed for spiro-OMeTAD produced a dramatic decrease of performance (Figure S28).

[20] This system has attained in average an efficiency 0.92 times the value for the reference samples prepared with doped spiro-OMeTAD. But it is important to highlight that a higher performing mixed perovskite with methylammonium and formamidinium organic cations and iodine and bromide anions was employed. S. Paek et al., , *Adv. Mater.* **2017**, 1606555.

[21] C. Huang, W. Fu, C.-Z. Li, Z. Zhang, W. Qiu, M. Shi, P. Heremans, A. K. Y. Jen, H. Chen, *J. Am. Chem. Soc.* **2016**, *138*, 2528-2531.

[22] A. Dualeh, T. Moehl, N. Tétreault, J. Teuscher, P. Gao, M. K. Nazeeruddin, M. Grätzel, *ACS Nano* **2014**, *8*, 362-373.

[23] H.-S. Kim, J.-W. Lee, N. Yantara, P. P. Boix, S. A. Kulkarni, S. Mhaisalkar, M. Grätzel, N.-G. Park, *Nano Lett.* **2013**, *16*, 2412-2417.

[24] J. Jiménez-López, W. Cambarau, L. Cabau, E. Palomares, *Sci. Rep.* **2017**, *7*, 6101.

[25] G. Xing, N. Mathews, S. Sun, S. S. Lim, Y. M. Lam, M. Grätzel, S. Mhaisalkar, T. C. Sum, *Science* **2013**, *342*, 344-347.

[26] D.-Y. Son et al., *Nat. Energy* **2016**, *1*, 16081.

[27] A. Fakharuddin, L. Schmidt-Mende, G. Garcia-Belmonte, R. Jose, I. Mora-Seró, *Adv. Energy Mater.* **2017**, 1700623.

[28] Y. Shao, Y. Yuan, J. Huang, *Nat. Energy* **2016**, *1*, 15001.

[29] S. Collavini, I. Kosta, S. F. Völker, G. Cabanero, H. J. Grande, R. Tena-Zaera, J. L. Delgado, *ChemSusChem* **2016**, *9*, 1263-1270.

[30] D. M. Guldi, N. Martin, *Fullerenes: From Synthesis to Optoelectronic Properties. Vol. 4*, Springer Netherlands, Dordrecht, **2002**..

[31] F. Langa, J.-F. Nierengarten, *Fullerenes. Principles and Applications*, RSC, Cambridge, **2007**.

10.1002/chem.201801069

WILEY-VCH

Entry for the Table of Contents (Please choose one layout)

Layout 1:

COMMUNICATION

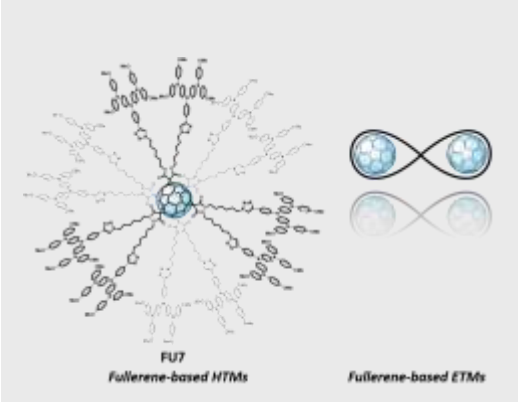

S. F. Völker, M. Vallés-Pelarda, J. Pascual, S. Collavini, F. Ruiperez, E. Zuccatti, L. E. Hueso, R. Tena-Zaera, I. Mora-Seró,* and J. L. Delgado**

Page No. – Page No.

Fullerene-Based Materials as Hole-Transporting/Electron Blocking Layers.

Applications in Perovskite Solar Cells